

Some numerical computations on real projective hypersurfaces

Jonathan D. Hauenstein* Emma L. Schmidt†

March 22, 2025

Abstract

For a smooth hypersurface defined by a homogeneous polynomial with real coefficients, algorithms are presented to determine the connected components and compute the Euler characteristic for both the real part of the hypersurface and its complement in real projective space. A bipartite graph, which describes the boundary relationships amongst all connected components, is also computed, which, for example, can be used to determine if a connected component of the real hypersurface is one-sided or two-sided. For curves, the nesting structure and dividing type are also considered. Several examples are used to demonstrate the numerical computations.

Keywords. Real hypersurfaces, nesting structure, Euler characteristic, real algebraic sets, polynomial systems, real numerical algebraic geometry, numerical algebraic geometry

1 Introduction

A classical problem in real algebraic geometry is to determine the topological types of smooth curves in the real projective plane $\mathbb{P}_{\mathbb{R}}^2$. For instance, Hilbert's 16th problem asks to classify the topological types for smooth curves of degree d , which has been solved for $d \leq 7$, and similarly for surfaces, e.g., see surveys [12, 14] and the many references therein. Harnack's curve theorem [6], the foundation for this problem from Hilbert, posits that the maximum number of connected components of the real part of curve of degree d in the real projective plane is $1 + \binom{d-1}{2}$, and this bound is sharp.

Rather than provide new theoretical results about Hilbert's 16th problem in general, the aim of this paper is to describe how to perform explicit computations associated with real projective hypersurfaces. For a real hypersurface $H \subset \mathbb{P}_{\mathbb{R}}^n$, the first computation determines the connected components of H and $\mathbb{P}_{\mathbb{R}}^n \setminus H$ and corresponding Euler characteristics. Then, for each connected component of $\mathbb{P}_{\mathbb{R}}^n \setminus H$, one can determine which connected components of H are contained in its boundary. Such relationships between the connected components of a real hypersurface and its complement can be represented by a bipartite graph, called a *connectivity graph*. In particular, a connectivity graph can be used to determine which connected components of the real hypersurface divides $\mathbb{P}_{\mathbb{R}}^n$ into two connected components, called *two-sided*, or does not divide $\mathbb{P}_{\mathbb{R}}^n$, called *one-sided*. See [11] for more details about the mutual position of hypersurfaces in $\mathbb{P}_{\mathbb{R}}^n$. In fact, for the curve case, the two-sided components are called *ovals* and the connectivity graph can be used to determine the nesting structure of ovals via Theorem 3.8. Figure 1 illustrates the connectivity

*Department of Applied and Computational Mathematics and Statistics, University of Notre Dame, Notre Dame, IN 46556 (hauenstein@nd.edu, <https://www.nd.edu/~jhauenst>)

†Department of Applied and Computational Mathematics and Statistics, University of Notre Dame, Notre Dame, IN 46556 (eschmi23@nd.edu)

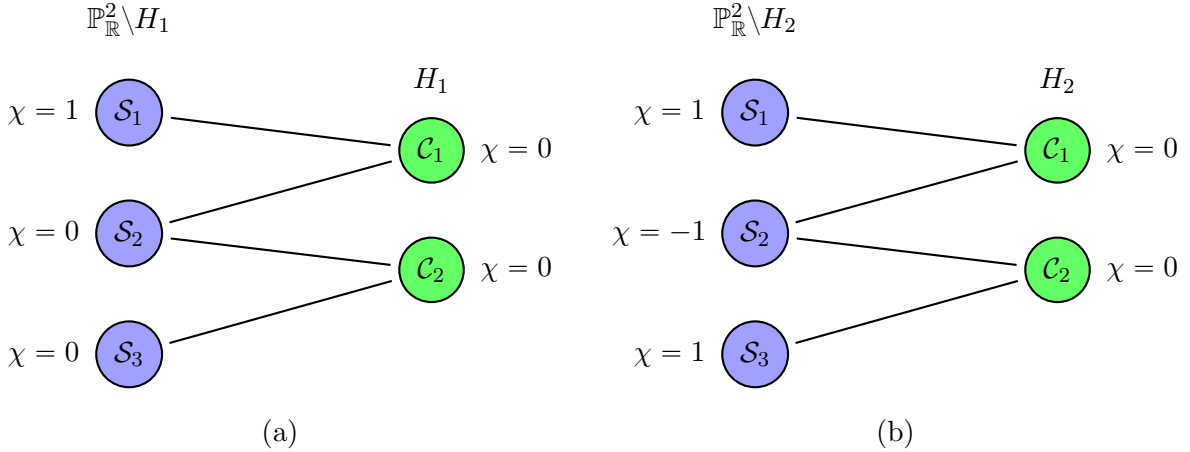


Figure 1: Connectivity graph for two curves, H_1 and H_2 , in the real projective plane with each having 2 two-sided connected components, i.e., two ovals. (a) Ovals in H_1 are nested since \mathcal{C}_1 is contained in the inside of \mathcal{C}_2 . (b) Ovals in H_2 are not nested since the inside of the ovals \mathcal{C}_1 and \mathcal{C}_2 , namely \mathcal{S}_1 and \mathcal{S}_3 , respectively, do not intersect.

graph for two curves in $\mathbb{P}_{\mathbb{R}}^2$, each having two ovals \mathcal{C}_1 and \mathcal{C}_2 . In Figure 1(a), the two ovals are nested with \mathcal{C}_1 nested in \mathcal{C}_2 . However, the connectivity graph in Figure 1(b) shows that ovals \mathcal{C}_1 and \mathcal{C}_2 in H_2 are not nested.

Let $f \in \mathbb{R}[x_0, x_1, x_2]$ be homogeneous and consider the corresponding complex and real curves:

$$C(f) = \{x \in \mathbb{P}^2 \mid f(x) = 0\} \quad \text{and} \quad C_{\mathbb{R}}(f) = C(f) \cap \mathbb{P}_{\mathbb{R}}^2 = \{x \in \mathbb{P}_{\mathbb{R}}^2 \mid f(x) = 0\}. \quad (1)$$

The case of interest below is when the algebraic curve $C(f)$ is smooth. Then, one can view $C(f)$ as a Riemann surface with $C_{\mathbb{R}}(f)$ being a curve on this surface. The polynomial f is said to be *non-dividing* if $C(f) \setminus C_{\mathbb{R}}(f)$ is connected, and *dividing* otherwise. Theorem 4.1 and Corollary 4.3 describe computational approaches to compute the dividing type of f using Whitney’s embedding [13] of \mathbb{P}^2 into \mathbb{R}^7 , which addresses a problem stated in [7].

The key to the algorithms presented below is the recently developed approach for computing the smoothly connected components of a real algebraic variety described in [5]. In particular, this approach uses a *routing function* to represent each smoothly connected component with a finite set of critical points, called *routing points*, along with a finite set of gradient ascent/descent paths between the critical points, called *routing paths*. The Euler characteristic of each connected component naturally arises as the alternating sum from the indices of the corresponding routing points.

Since studying real projective hypersurfaces is such a classical problem, many approaches have been utilized. The following summarizes a few related approaches. In [7], curves of degree six in the real projective plane are investigated via a cylindrical algebraic decomposition (CAD)—see [3] for a general overview, which can be computed efficiently for plane curves [4]. A computational approach based on homology basis is described in [8]. Although not a computational approach, we note that statistics on the number of connected components was considered in [9].

The rest of the paper is organized as follows. Section 2 contains background information about routing functions and computing connected components. Section 3 considers connectivity graphs and, for the curve case, the nesting of ovals. Section 4 considers computing the dividing type for curves. Examples are presented in Section 5, and short conclusion is provided in Section 6.

2 Hypersurfaces, routing functions, and connectivity

The following provides necessary background information regarding hypersurfaces, n -spheres, routing functions, and connectivity. For general details about real algebraic geometry, see, e.g., [1, 3].

2.1 Hypersurfaces and spheres

Suppose that $f \in \mathbb{R}[x_0, \dots, x_n]$ is homogeneous of degree $d \geq 1$ such that the *hypersurface defined by f* , namely

$$V_{\mathbb{P}}(f) = \{x \in \mathbb{P}^n \mid f(x) = 0\},$$

is *smooth*, i.e.,

$$V_{\mathbb{P}}(\nabla f) = \bigcap_{i=0}^n V_{\mathbb{P}}\left(\frac{\partial f}{\partial x_i}\right) = \emptyset$$

where ∇f is the gradient of f . When $n = 2$, $V_{\mathbb{P}}(f)$ is called a *curve* while $V_{\mathbb{P}}(f)$ is called a *surface* when $n = 3$.

Example 2.1 *The curve defined with $f = x_0x_1 - x_2^2$, which is a parabola, is smooth since*

$$x_1 = x_0 = -2x_2 = 0$$

has no solutions in \mathbb{P}^2 . However, the curve defined by $g = x_1^2 - x_2^2$, which consists of two intersecting lines, is not smooth with a singularity at $[1, 0, 0] \in \mathbb{P}^2$.

One approach to perform computations on $\mathbb{P}_{\mathbb{R}}^n$ is to perform computations on the n -sphere

$$\mathbb{S}^n = \{x \in \mathbb{R}^{n+1} \mid x_0^2 + \dots + x_n^2 - 1 = 0\}$$

which naturally provides a double cover of $\mathbb{P}_{\mathbb{R}}^n$ by identifying antipodal points. In particular, define

$$V_{\mathbb{S}}(f) = \{x \in \mathbb{S}^n \mid f(x) = 0\}.$$

Throughout, we will utilize

$$S(x) = x_0^2 + \dots + x_n^2 - 1 \tag{2}$$

and corresponding complex and real varieties, respectively:

$$V_{\mathbb{C}}(f, S) = \{x \in \mathbb{C}^{n+1} \mid f(x) = 0, S(x) = 0\} \quad \text{and} \quad V_{\mathbb{R}}(f, S) = \{x \in \mathbb{R}^{n+1} \mid f(x) = 0, S(x) = 0\}. \tag{3}$$

Example 2.2 *Continuing with Example 2.1, Figure 2 plots $V_{\mathbb{R}}(f, S)$ and $V_{\mathbb{R}}(g, S)$. In particular, $V_{\mathbb{R}}(f, S)$ is smooth while $V_{\mathbb{R}}(g, S)$ has a singularity.*

Another approach to perform computations on both $\mathbb{P}_{\mathbb{R}}^n$ and \mathbb{P}^n simultaneously is to utilize an embedding into a suitable real affine space, e.g., Whitney's embedding [13]. For $\mathbb{P}_{\mathbb{R}}^n$, this avoids having to identify antipodal points at the cost of having to compute images under the embedding and then perform additional computations in an ambient space of higher dimension. Thus, Section 3 will perform computations in $\mathbb{P}_{\mathbb{R}}^2$ using the double cover provided by \mathbb{S}^2 . However, since Section 4 considers $C(f) \setminus C_{\mathbb{R}}(f)$ where $C(f) \subset \mathbb{P}^2$ and $C_{\mathbb{R}}(f) \subset \mathbb{P}_{\mathbb{R}}^2$, we utilize Whitney's embedding [13] to compute the connected components of $C(f) \setminus C_{\mathbb{R}}(f)$ via computations performed in \mathbb{R}^7 .

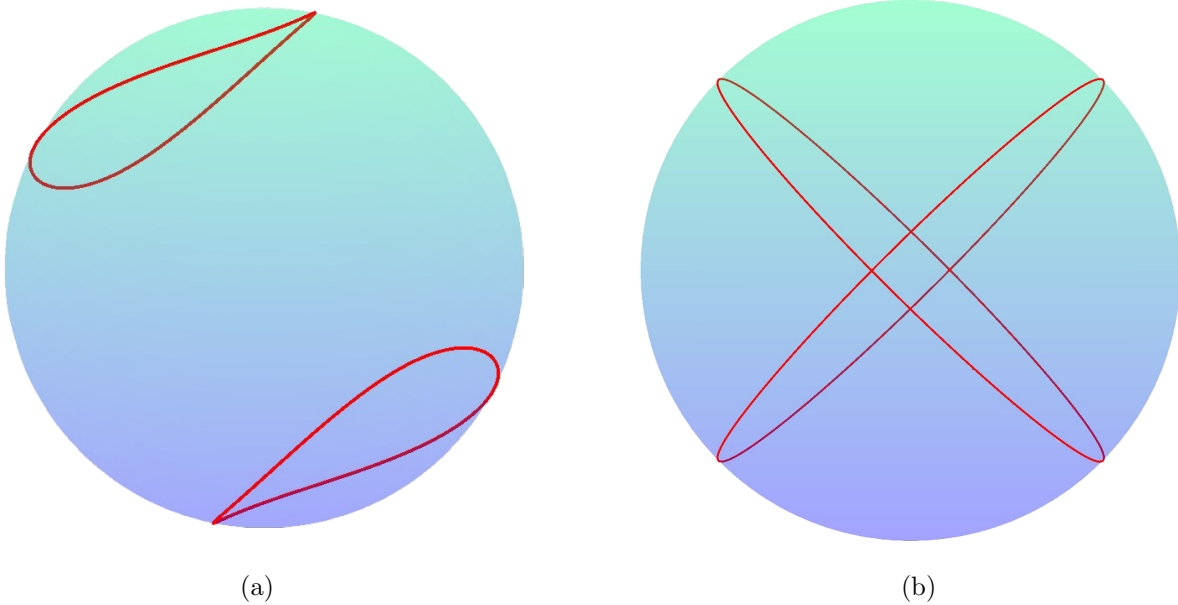


Figure 2: Plot of (a) parabola on unit sphere and (b) two intersecting lines on unit sphere.

2.2 Routing functions, Euler characteristic, and membership testing

Since all computations related to connected components will be performed on a subset in some real affine space, suppose that $F = \{f_1, \dots, f_\ell\} \subset \mathbb{R}[x_1, \dots, x_n]$ is a collection of polynomials where $V_{\mathbb{C}}(F)$ is pure-dimensional of codimension k and $V_{\mathbb{R}}(F)$ is a smooth subset of $V_{\mathbb{C}}(F)$. That is, $\text{rank } J(x) = k$ for every $x \in V_{\mathbb{R}}(F)$ where $J(x)$ is the $\ell \times n$ Jacobian matrix of F evaluated at x . Given a nonzero polynomial $g \in \mathbb{R}[x_1, \dots, x_n]$, the key computation is to determine the connected components of $X = V_{\mathbb{R}}(F) \setminus V_{\mathbb{R}}(F, g)$. For example, if $g(x) \equiv 1$, then $V_{\mathbb{R}}(F, g) = \emptyset$ so that one simply computes the connected components of $V_{\mathbb{R}}(F)$. Although [5] considers smoothly connected components, *connected* and *smoothly connected* are equivalent here based on the smoothness assumption on $V_{\mathbb{R}}(F)$. In particular, as in [5], the connected components of X will be computed using a *routing function* $r(x)$ so that each connected component of X is represented by a finite set of points, called *routing points*, that are connected via a finite set of gradient ascent/descent paths associated with $r(x)$ on X , called *routing paths*. Each routing point has an *index* associated with r on X and the Euler characteristic of the connected component is simply the alternating sum from the indices of the corresponding routing points, i.e., even index contributes $+1$ and odd index contributes -1 . Routing paths emanate along the unstable eigenvector directions at each routing point.

Let $c \in \mathbb{R}^n$ and $d \in \mathbb{Z}_{>0}$ such that $2d > \deg g$. As in [5], the routing function used here is

$$r(x) = \frac{g(x)}{(1 + (x_1 - c_1)^2 + \dots + (x_n - c_n)^2)^d}. \quad (4)$$

By [5, Thm. 3.4], r is a routing function on X for a Zariski open dense subset of $c \in \mathbb{R}^n$. In particular, we assume that a random number generator used to select $c \in \mathbb{R}^n$ will yield an element in this Zariski open dense subset with *probability one*. The routing points of r on X are simply the critical points of r on X , that is, satisfy

$$x \in X \quad \text{with} \quad \text{rank} \begin{bmatrix} \nabla r(x) \\ J(x) \end{bmatrix} = k.$$

Since X is smooth, there is a well-defined gradient $\nabla_X r$ of r on X and the routing points of r on X are precisely where $\nabla_X r = 0$ on X . A routing function has finitely many routing points on X and each is nondegenerate, i.e., the corresponding $(n - k) \times (n - k)$ Hessian matrix of r on X , denoted $H_X r$, is invertible at each routing point of r on X . Moreover, the index of a routing point x is the number of eigenvalues of $H_X r(x)$ which have the same sign as $r(x)$. Eigenvalues of $H_X r(x)$ with the same sign as $r(x)$ are called *unstable eigenvalues* and the corresponding eigenvectors are called *unstable eigenvectors*. For instance, if x is a routing point with $r(x) > 0$, then the index of x is the number of positive eigenvalues so that, in particular, a local maximum has index 0.

The final piece is to partition the routing points into subsets which lie on the same connected component of X . This is accomplished using gradient ascent (when $r > 0$)/descent (when $r < 0$) paths of r on X starting at the routing points of positive index along the unstable eigenvector directions. In particular, suppose that x is a routing point and v is an unstable eigenvector. Then, for every $\epsilon > 0$, the solution $z_\epsilon(t)$ to

$$\begin{aligned} \dot{z}(t) &= \text{sign}(r(x)) \cdot \nabla_X r(z) \\ z(0) &= x + \epsilon \cdot v \end{aligned} \tag{5}$$

is well-defined. Moreover, the routing path $z(t) = \lim_{\epsilon \rightarrow 0^+} z_\epsilon(t)$ is also well-defined which starts ($t = 0$) at x and ends ($t = \infty$) at another routing point on the same connected component of X . One also obtains a routing path associated with $-v$ which may or may not end at the same routing point as the one associated with v . Thus, looping over routing points and corresponding unstable eigenvectors v and $-v$, one obtains a finite collection of routing paths which yields the same connectivity structure as the connected components of X . This is summarized in Algorithm 1 which arises from [5, Alg. 1] and is justified by [5, Thm. 4.4].

Example 2.3 For $f(x) = x_0 x_1 - x_2^2$ as in Example 2.1 and $S(x) = x_0^2 + x_1^2 + x_2^2 - 1$, the following illustrates using Algorithm 1 to compute the connected components of $V_{\mathbb{R}}(f, S)$ and the connected components of $V_{\mathbb{R}}(S) \setminus V_{\mathbb{R}}(f, S)$. For simplicity of presentation, fix $c = (1/2, -1/3, -1/5)$. The number of routing points depends on the choice of c , but, of course, the corresponding Euler characteristics are independent of c .

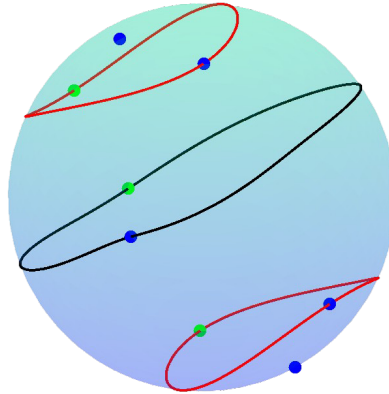


Figure 3: Plot of parabola defined by $f = x_0 x_1 - x_2^2$ (red) on the unit sphere \mathbb{S}^2 . Routing points for the parabola $V_{\mathbb{R}}(f, S)$ and complement of the parabola $V_{\mathbb{R}}(S) \setminus V_{\mathbb{R}}(f, S)$ are shown with blue points having index 0 and green points having index 1. Routing paths for the complement are black.

Input: A collection of polynomials $F = \{f_1, \dots, f_\ell\} \subset \mathbb{R}[x_1, \dots, x_n]$ such that $V_{\mathbb{C}}(F)$ is pure-dimensional and $V_{\mathbb{R}}(F)$ is a smooth subset of $V_{\mathbb{C}}(F)$, and routing function r .

Output: Euler characteristic of $X = V_{\mathbb{R}}(F) \setminus V_{\mathbb{R}}(F, r)$ and partitioned subset of the routing points of r on X corresponding to the connected components of X .

- 1 Compute the routing points of r on X , say p_1, \dots, p_m , and corresponding indices, say i_1, \dots, i_m .
- 2 Compute $\chi = \sum_{j=1}^m (-1)^{i_j}$.
- 3 Initialize $A = I_m$, the $m \times m$ identity matrix.
- 4 **for** $j = 1, \dots, m$ **do**
- 5 **foreach** *unstable eigenvector* v for $H_X r(p_j)$ **do**
- 6 Compute limit routing point from p_j in the direction v with respect to r , say p_{w_+} .
- 7 Set $A_{jw_+} = A_{w_+j} = 1$.
- 8 Compute limit routing point from p_j in the direction $-v$ with respect to r , say p_{w_-} .
- 9 Set $A_{jw_-} = A_{w_-j} = 1$.
- 10 **end**
- 11 **end**
- 12 Set M to be the transitive closure of A .
- 13 Partition $\{p_1, \dots, p_m\}$ based on the connected components of M , say C_1, \dots, C_s .
- 14 **for** $j = 1, \dots, s$ **do**
- 15 Compute $\chi_j = \sum_{a=1}^m \mathbf{1}_{p_a \in C_j} \cdot (-1)^{i_a}$ where $\mathbf{1}_{y \in W} = \begin{cases} 1 & y \in W \\ 0 & y \notin W \end{cases}$.
- 16 **end**
- 17 **return** $(\chi, \{\{C_1, \chi_1\}, \dots, \{C_s, \chi_s\}\})$

Algorithm 1: Euler characteristic and connected components

For $V_{\mathbb{R}}(f, S)$, one can take the routing function $r(x) = (1 + (x_0 - c_0)^2 + (x_1 - c_1)^2 + (x_2 - c_2)^2)^{-1}$. Since $V_{\mathbb{R}}(f, S, r) = \emptyset$, $X = V_{\mathbb{R}}(f, S)$ as in Algorithm 1. There are four routing points of r on X , two each of index 0 and index 1 so that $\chi = 0$ as expected. To four decimal places, we have

$$p_1 = (0.9861, 0.0272, -0.1638), \quad p_2 = (-0.0214, -0.9891, -0.1455), \quad p_3 = -p_1, \quad p_4 = -p_2,$$

with corresponding indices $i_1 = i_2 = 0$ and $i_3 = i_4 = 1$. Both unstable directions from p_3 end at p_2 and similarly for p_4 ending at p_1 yielding the connectivity matrix

$$M = \begin{bmatrix} 1 & 0 & 0 & 1 \\ 0 & 1 & 1 & 0 \\ 0 & 1 & 1 & 0 \\ 1 & 0 & 0 & 1 \end{bmatrix}.$$

Hence, Algorithm 1 obtains two connected components of X corresponding to $C_1 = \{p_1, p_4\}$ with $\chi_1 = 0$ and $C_2 = \{p_2, p_3\}$ with $\chi_2 = 0$. Figure 3 shows these four routing points on $V_{\mathbb{R}}(f, S)$ with the routing paths simply tracing out $V_{\mathbb{R}}(f, S)$.

For $V_{\mathbb{R}}(S) \setminus V_{\mathbb{R}}(f, S)$, one can take the routing function

$$r(x) = \frac{x_0 x_1 - x_2^2}{(1 + (x_0 - c_0)^2 + (x_1 - c_1)^2 + (x_2 - c_2)^2)^2}$$

with $X = V_{\mathbb{R}}(S) \setminus V_{\mathbb{R}}(S, r) = V_{\mathbb{R}}(S) \setminus V_{\mathbb{R}}(f, S)$. There are four routing points of r on X , three of index 0 and one of index 1 so that $\chi = 2$ as expected. To four decimal places, we have

$$\begin{aligned} p_1 &= (0.8646, 0.4989, -0.0596), & p_2 &= (0.5992, -0.4977, -0.6271), \\ p_3 &= (-0.6762, 0.7319, 0.0839), & p_4 &= (-0.5214, -0.8517, -0.0520), \end{aligned}$$

with corresponding indices $i_1 = i_2 = i_4 = 0$ and $i_3 = 1$. Both unstable directions from p_3 end at p_2 yielding the connectivity matrix

$$M = \begin{bmatrix} 1 & 0 & 0 & 0 \\ 0 & 1 & 1 & 0 \\ 0 & 1 & 1 & 0 \\ 0 & 0 & 0 & 1 \end{bmatrix}.$$

Hence, Algorithm 1 obtains three connected components of X corresponding to $C_1 = \{p_1\}$ with $\chi_1 = 1$, $C_2 = \{p_2, p_3\}$ with $\chi_2 = 0$, and $C_3 = \{p_4\}$ with $\chi_3 = 1$. Figure 3 shows these four routing points on $V_{\mathbb{R}}(S) \setminus V_{\mathbb{R}}(f, S)$ together with the routing paths.

Given a point $y \in X$, the output of Algorithm 1 can be used to determine which connected component contains y . Of course, if y is a routing point, membership is trivial so assume that y is not a routing point. Adapting (5) yields

$$\begin{aligned} \dot{z}(t) &= \text{sign}(r(y)) \cdot \nabla_X r(z) \\ z(0) &= y \end{aligned} \tag{6}$$

where the routing point $x = \lim_{t \rightarrow \infty} z(t)$ and y are in the same connected component [5, Thm. 4.4].

Remark 2.4 One way in which membership testing will be used is to test which components are identified under the antipodal action on \mathbb{S}^n . Suppose that $F = \{f_1, \dots, f_\ell\} \subset \mathbb{R}[x_0, \dots, x_n]$ is a collection of homogeneous polynomials and S as in (2) such that $V_{\mathbb{C}}(F, S)$ is pure-dimensional and $V_{\mathbb{R}}(F, S)$ is a smooth subset of $V_{\mathbb{C}}(F, S)$. Let $g \in \mathbb{R}[x_0, \dots, x_n]$ be nonzero and homogeneous. Then, $X = V_{\mathbb{R}}(F, S) \setminus V_{\mathbb{R}}(F, S, g)$ is invariant under the antipodal action, i.e., $-x \in X$ if and only if $x \in X$. Moreover, membership testing permits identifying the orbits of the connected components of X under the antipodal action. For a connected component of X , one simply selects a corresponding routing point x and applies membership testing to its antipodal point $-x$. If x and $-x$ lie in the same connected component, then that component is invariant under the antipodal action. Otherwise, x and $-x$ lie on two different connected components which are identified under the antipodal action.

Example 2.5 From Example 2.3, the routing points associated with $V_{\mathbb{R}}(f, S)$ are antipodal and thus the corresponding components C_1 and C_2 are identified under the antipodal action.

For $V_{\mathbb{R}}(S) \setminus V_{\mathbb{R}}(f, S)$, membership testing using (6) starting at $-p_1$ yields p_4 showing that C_1 and C_3 are identified under the antipodal action. However, starting at $-p_2$ yields p_2 showing that C_2 is invariant under the antipodal action.

3 Connectivity graphs and topological type

Building on the computational approaches described in Section 2, the following first considers the case where $f \in \mathbb{R}[x_0, x_1, x_2]$ is nonconstant and homogeneous such that $C(f)$ as in (1) is smooth. In particular, for $C_{\mathbb{R}}(f) \subset \mathbb{P}_{\mathbb{R}}^2$, Section 3.1 considers determining the connected components

of $C_{\mathbb{R}}(f)$ and $\mathbb{P}_{\mathbb{R}}^2 \setminus C_{\mathbb{R}}(f)$ along with computing a bipartite graph, called a *connectivity graph*, that describes which connected components of $C_{\mathbb{R}}(f)$ lie in the boundary of each connected component of $\mathbb{P}_{\mathbb{R}}^2 \setminus C_{\mathbb{R}}(f)$. Remark 3.7 highlights that all such computations, including the connectivity graph, can be trivially extended to $\mathbb{P}_{\mathbb{R}}^n$ with examples presented in Section 5.1.

Section 3.2 uses the connectivity graph associated with f in $\mathbb{P}_{\mathbb{R}}^2$ to determine the *nesting structure* of the ovals in $C_{\mathbb{R}}(f) \subset \mathbb{P}_{\mathbb{R}}^2$ yielding its *topological type*.

3.1 Connectivity graph

For a randomly selected value $c \in \mathbb{R}^3$, as illustrated in Example 2.3, Algorithm 1 can be applied to compute the connected components of $V_{\mathbb{R}}(f, S) \subset \mathbb{S}^2$ using the routing function

$$r_1(x) = \frac{1}{(1 + (x_0 - c_0)^2 + (x_1 - c_1)^2 + (x_2 - c_2)^2)},$$

say $\mathcal{C}_1, \dots, \mathcal{C}_s$. Similarly, the connected components of $\mathbb{S}^2 \setminus V_{\mathbb{R}}(f) = V_{\mathbb{R}}(S) \setminus V_{\mathbb{R}}(f, S)$ can be computed using the routing function

$$r_2(x) = \frac{f(x)}{(1 + (x_0 - c_0)^2 + (x_1 - c_1)^2 + (x_2 - c_2)^2)^d}$$

where $2d > \deg f$, say $\mathcal{S}_1, \dots, \mathcal{S}_t$. Even though \mathbb{S}^2 is compact, the denominators are used to provide enough genericity to ensure that both r_1 and r_2 are routing functions for a randomly selected $c \in \mathbb{R}^3$ with probability one [5].

One way to describe the relationship between $\mathcal{C}_1, \dots, \mathcal{C}_s$ and $\mathcal{S}_1, \dots, \mathcal{S}_t$ is via a bipartite graph, called a *connectivity graph*, with the two parts of size s and t corresponding with $\mathcal{C}_1, \dots, \mathcal{C}_s$ and $\mathcal{S}_1, \dots, \mathcal{S}_t$, respectively. The edges of this graph are determined based on whether \mathcal{C}_i is contained in the boundary of \mathcal{S}_j .

To avoid some subscripts, suppose that \mathcal{C} is a connected component of $V_{\mathbb{R}}(f, S)$ and $x \in \mathcal{C}$ is a routing point with respect to r_1 . Select a plane $\mathcal{P} \subset \mathbb{R}^3$ passing through the origin and x such that \mathcal{P} intersects $V_{\mathbb{R}}(f, S)$ transversely, which is an open condition. In particular, the points in $V_{\mathbb{R}}(f, S) \cap \mathcal{P}$, say p_1, \dots, p_u , can be cyclically ordered around the circle $\mathbb{S}^2 \cap \mathcal{P}$ with $p_1 = x = p_{u+1}$ as illustrated in Figure 4. Therefore, every point on the open arc on the circle $\mathbb{S}^2 \cap \mathcal{P}$ between p_1 and p_2 , denoted (p_1, p_2) , lies in the same connected component of $V_{\mathbb{R}}(S) \setminus V_{\mathbb{R}}(f, S)$ and similarly for the arc between p_u and p_1 , denoted (p_u, p_1) . Hence, one simply selects $y \in (p_1, p_2) \in V_{\mathbb{R}}(S) \setminus V_{\mathbb{R}}(f, S)$ and applies membership testing to determine the value of j such that $y \in \mathcal{S}_j$. Similarly, one repeats for $y' \in (p_u, p_1)$ to determine the value of j' such that $y' \in \mathcal{S}_{j'}$. This process is summarized in Algorithm 2 with the following verifying correctness.

Theorem 3.1 *Algorithm 3.1 correctly determines the connectivity graph associated to f in \mathbb{S}^2 with probability one.*

Proof. In Step 4 of Algorithm 2, a random plane is transverse to $V_{\mathbb{R}}(f, S)$ with probability one. In Step 6 of Algorithm 2, since the open arc $(p_1, p_2) \subset V_{\mathbb{R}}(S) \setminus V_{\mathbb{R}}(f, S)$ is connected, every point in this open arc must be contained in the same connected component of $V_{\mathbb{R}}(S) \setminus V_{\mathbb{R}}(f, S)$, say \mathcal{S}_j . Since $x = p_1 \in V_{\mathbb{R}}(f, S)$, it immediately follows that x must be contained in the boundary of $\mathcal{S}_j \subset V_{\mathbb{R}}(S) \setminus V_{\mathbb{R}}(f, S)$. Since both \mathcal{C}_i and \mathcal{S}_j are smooth and connected, it follows that \mathcal{C}_i must therefore also be contained in the boundary of \mathcal{S}_j . One simply repeats this argument for Step 8. Smoothness and connectivity ensure that there can be no other connected component of $V_{\mathbb{R}}(S) \setminus V_{\mathbb{R}}(f, S)$ whose boundary contains \mathcal{C}_i besides \mathcal{S}_j and $\mathcal{S}_{j'}$. \square

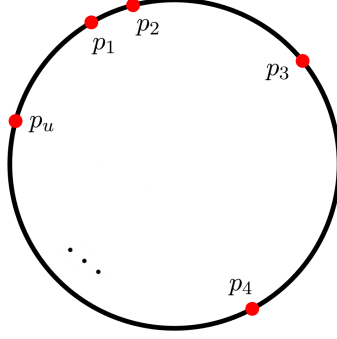


Figure 4: Illustrating cyclical ordering of points around a circle.

Input: Homogeneous polynomial $f \in \mathbb{R}[x_0, x_1, x_2]$ such that $V_{\mathbb{C}}(f, S)$ is irreducible of codimension 2 and $V_{\mathbb{R}}(f, S)$ is smooth where $S = x_0^2 + x_1^2 + x_2^2 - 1$, routing functions r_1 for $V_{\mathbb{R}}(f, S)$ and r_2 for $V_{\mathbb{R}}(S) \setminus V_{\mathbb{R}}(f, S)$, and corresponding partitioned subsets of routing points $\{C_1, \dots, C_s\}$ for $V_{\mathbb{R}}(f, S)$ and $\{S_1, \dots, S_t\}$ for $V_{\mathbb{R}}(S) \setminus V_{\mathbb{R}}(f, S)$ associated with connected components $\{C_1, \dots, C_s\}$ and $\{S_1, \dots, S_t\}$, respectively.

Output: Bipartite graph with the two parts corresponding to the connected components of $V_{\mathbb{R}}(f, S)$ and the connected components of $V_{\mathbb{R}}(S) \setminus V_{\mathbb{R}}(f, S)$ with edges determined based on if C_i is contained in the boundary of S_j .

- 1 Initialize an $s \times t$ matrix G with all entries 0.
- 2 **for** $j = 1, \dots, s$ **do**
- 3 Select a routing point $x \in C_j$.
- 4 Select a random plane $\mathcal{P} \subset \mathbb{R}^3$ passing through the origin and x .
- 5 Compute the points in $V_{\mathbb{R}}(f, S) \cap \mathcal{P}$, say p_1, \dots, p_u , which are ordered cyclically around the circle $S^2 \cap \mathcal{P}$ with $x = p_1 = p_{u+1}$.
- 6 Select the midpoint of the arc (p_1, p_u) , say y , and perform membership testing using r_2 to determine j' such that $y \in S_{j'}$.
- 7 Set $G_{jj'} = 1$.
- 8 Select the midpoint of the arc (p_u, p_1) , say y' , and perform membership testing using r_2 to determine j'' such that $y' \in S_{j''}$.
- 9 Set $G_{jj''} = 1$.
- 10 **end**
- 11 **return** bipartite graph associated with matrix G

Algorithm 2: Connectivity graph in \mathbb{S}^2

Remark 3.2 Membership testing on $V_{\mathbb{R}}(S) \setminus V_{\mathbb{R}}(f, S)$ can be performed using spherical coordinates so that ∇_X in (6) is transformed into a standard unconstrained gradient in spherical coordinates. Of course, a similar statement holds when there is a known global analytic parameterization.

Example 3.3 With the setup from Example 2.3, let C_1 and C_2 denoted the two connected components of $V_{\mathbb{R}}(f, S)$ and S_1, S_2 , and S_3 denote the three connected components of $V_{\mathbb{R}}(S) \setminus V_{\mathbb{R}}(f, S)$. Using Algorithm 1, one determines that C_1 is in the boundary of both S_1 and S_2 , and C_2 is in the

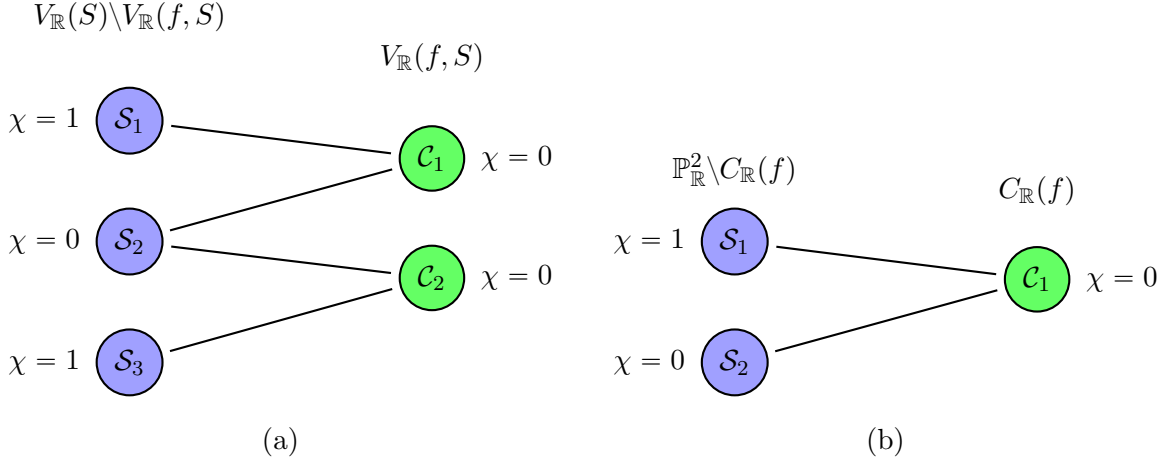


Figure 5: Bipartite connectivity graph arising in (a) \mathbb{S}^2 for Example 3.3 and (b) $\mathbb{P}_{\mathbb{R}}^2$ for Example 3.5.

boundary of both S_2 and S_3 . This yields the corresponding matrix

$$G = \begin{bmatrix} 1 & 1 & 0 \\ 0 & 1 & 1 \end{bmatrix}$$

with corresponding bipartite connectivity graph shown in Figure 5(a).

To determine the corresponding bipartite connectivity graph in $\mathbb{P}_{\mathbb{R}}^2$, one simply needs to identify the corresponding components in \mathbb{S}^2 under the antipodal action using Remark 2.4. This is summarized in Algorithm 3 with the following verifying correctness.

Theorem 3.4 *With probability one, Algorithm 3 correctly determines the bipartite connectivity graph associated with $C_{\mathbb{R}}(f)$ and $\mathbb{P}_{\mathbb{R}}^2 \setminus C_{\mathbb{R}}(f)$ and corresponding Euler characteristics.*

Proof. The functions r_1 and r_2 are routing functions associated with $V_{\mathbb{R}}(f, S)$ and $V_{\mathbb{R}}(S) \setminus V_{\mathbb{R}}(f, S)$, respectively, with probability one by [5, Thm. 3.4]. The rest follows from Theorem 3.1 and the relationship between \mathbb{S}^2 and $\mathbb{P}_{\mathbb{R}}^2$. \square

From the output of Algorithm 3, if a connected component \mathcal{C} of $C_{\mathbb{R}}(f)$ is contained in the boundary of two different connected components of $\mathbb{P}_{\mathbb{R}}^2 \setminus C_{\mathbb{R}}(f)$, then \mathcal{C} is called *two-sided* or an *oval*. Otherwise, it is called *one-sided* or a *pseudoline*. If f has even degree, all connected components of $C_{\mathbb{R}}(f)$ are ovals. There is exactly one pseudoline when f has odd degree and all other connected components of $C_{\mathbb{R}}(f)$ are ovals.

Example 3.5 *Continuing with Example 3.3, antipodal membership testing in Example 2.5 with Algorithm 3 produces $G = \begin{bmatrix} 1 & 1 \end{bmatrix}$ with corresponding connectivity graph shown in Figure 5(b).*

Example 3.6 *Applying Algorithm 3 to $f(x) = x_0x_2^2 - x_1^3 + 2x_0^2x_1$ yields the connectivity graph displayed in Figure 6. In particular, $C_{\mathbb{R}}(f)$ consists of one oval \mathcal{C}_1 and one pseudoline \mathcal{C}_2 .*

Input: Nonconstant homogeneous polynomial $f \in \mathbb{R}[x_0, x_1, x_2]$ such that $C(f)$ is smooth.

Output: Bipartite graph with the two parts corresponding to the connected components of $C_{\mathbb{R}}(f)$ and the connected components of $\mathbb{P}_{\mathbb{R}}^2 \setminus C_{\mathbb{R}}(f)$ with edges determined based on if a connected component of $C_{\mathbb{R}}(f)$ is contained in the boundary of a connected component of $\mathbb{P}_{\mathbb{R}}^2 \setminus C_{\mathbb{R}}(f)$, and corresponding Euler characteristics.

1 Randomly select $c \in \mathbb{R}^3$ and construct functions

$$r_1(x) = (1 + (x_0 - c_0)^2 + (x_1 - c_1)^2 + (x_2 - c_2)^2)^{-1} \quad \text{and} \quad r_2(x) = f(x) \cdot r_1(x)^d$$

where $d = \lceil \deg f/2 \rceil > 0$. Construct $S(x) = x_0^2 + x_1^2 + x_2^2 - 1$.

2 Apply Algorithm 1 to $\{f, S\}$ with r_1 yielding the connected components of $V_{\mathbb{R}}(f, S)$.

3 Apply Algorithm 1 to $\{S\}$ with r_2 yielding the connected components of $V_{\mathbb{R}}(S) \setminus V_{\mathbb{R}}(f, S)$.

4 Apply Algorithm 2 yielding the connectivity graph G associated with $V_{\mathbb{R}}(f, S)$ and $V_{\mathbb{R}}(S) \setminus V_{\mathbb{R}}(f, S)$ in \mathbb{S}^2 .

5 Set E to be the set whose elements are the connected components of $V_{\mathbb{R}}(f, S)$.

6 **while** $E \neq \emptyset$ **do**

7 Select \mathcal{C} from E and set $E = E \setminus \{\mathcal{C}\}$.

8 Select a routing point $x \in \mathcal{C}$ and perform a membership test with $-x$ to determine connected component \mathcal{C}' of $V_{\mathbb{R}}(f, S)$ containing $-x$.

9 **if** $\mathcal{C} \neq \mathcal{C}'$ **then**

10 Set $E = E \setminus \{\mathcal{C}'\}$.

11 Merge the vertices in G corresponding with \mathcal{C} and \mathcal{C}' and set the corresponding Euler characteristic of \mathcal{C} in $\mathbb{P}_{\mathbb{R}}^2$ to $\chi(\mathcal{C}) = \chi(\mathcal{C}') = (\chi(\mathcal{C}) + \chi(\mathcal{C}'))/2$.

12 **else**

13 Set the corresponding Euler characteristic of \mathcal{C} in $\mathbb{P}_{\mathbb{R}}^2$ to $\chi(\mathcal{C})/2$.

14 **end**

15 **end**

16 Set E to be the set whose elements are the connected components of $V_{\mathbb{R}}(S) \setminus V_{\mathbb{R}}(f, S)$.

17 **while** $E \neq \emptyset$ **do**

18 Select \mathcal{S} from E and set $E = E \setminus \{\mathcal{S}\}$.

19 Select a routing point $x \in \mathcal{S}$ and perform a membership test with $-x$ to determine connected component \mathcal{S}' of $V_{\mathbb{R}}(S) \setminus V_{\mathbb{R}}(f, S)$ containing $-x$.

20 **if** $\mathcal{S} \neq \mathcal{S}'$ **then**

21 Set $E = E \setminus \{\mathcal{S}'\}$.

22 Merge the vertices in G corresponding with \mathcal{S} and \mathcal{S}' and set the corresponding Euler characteristic of \mathcal{S} in $\mathbb{P}_{\mathbb{R}}^2$ to $\chi(\mathcal{S}) = \chi(\mathcal{S}') = (\chi(\mathcal{S}) + \chi(\mathcal{S}'))/2$.

23 **else**

24 Set the corresponding Euler characteristic of \mathcal{S} in $\mathbb{P}_{\mathbb{R}}^2$ to $\chi(\mathcal{S})/2$.

25 **end**

26 **end**

27 **return** bipartite graph associated with matrix G along with corresponding Euler characteristics

Algorithm 3: Connectivity graph in $\mathbb{P}_{\mathbb{R}}^2$

Remark 3.7 Since Euler characteristic and connected component decomposition computed in Al-

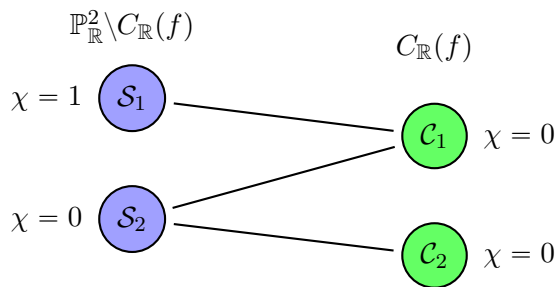


Figure 6: Bipartite connectivity graph arising in $\mathbb{P}_{\mathbb{R}}^2$ for Example 3.6.

Algorithm 1 applies in arbitrary dimensions, the computation of connectivity graphs in Algorithms 2 and 3 can be trivially extended to \mathbb{S}^n and $\mathbb{P}_{\mathbb{R}}^n$, respectively. In particular, the connectivity graph in $\mathbb{P}_{\mathbb{R}}^n$ arising from Algorithm 3 can be used to determine two-sidedness and one-sidedness.

3.2 Nesting of ovals and topological type

Each oval, which is two-sided, has an *inside* and an *outside*. The connectivity graph and corresponding Euler characteristics on $\mathbb{P}_{\mathbb{R}}^2$ computed by Algorithm 3 can be used to determine the Euler characteristic of the two sides. In fact, the inside is homeomorphic to a disk and has Euler characteristic 1, while the outside is homeomorphic to a Möbius strip with Euler characteristic 0.

Theorem 3.8 *Suppose that \mathcal{G} is the connectivity graph associated with $C_{\mathbb{R}}(f)$ computed from Algorithm 3. If \mathcal{C} is an oval in $C_{\mathbb{R}}(f)$, then removing the vertex corresponding with \mathcal{C} and two edges emanating from \mathcal{C} in \mathcal{G} yields a graph \mathcal{G}' with two connected components \mathcal{G}'_1 and \mathcal{G}'_2 . If X_1 and X_2 are the union of corresponding vertices in \mathcal{G}'_1 and \mathcal{G}'_2 respectively, then $\{\chi(X_1), \chi(X_2)\} = \{0, 1\}$. Upon relabeling, assume that $\chi(X_1) = 1$ and $\chi(X_2) = 0$. Then, $\mathcal{I} = X_1$ is the inside of \mathcal{C} and $\mathcal{O} = X_2$ is the outside of \mathcal{C} .*

Proof. Since \mathcal{C} is an oval, there is an inside and outside. In particular, $\mathbb{P}_{\mathbb{R}}^2 \setminus \mathcal{C}$ must have two connected components having Euler characteristics 0 and 1. Since the union of the corresponding vertices in \mathcal{G} is $\mathbb{P}_{\mathbb{R}}^2$, removing the vertex corresponding to \mathcal{C} shows that X_1 and X_2 are precisely the two connected components of $\mathbb{P}_{\mathbb{R}}^2 \setminus \mathcal{C}$. Since Euler characteristic is additive, $\chi(X_1)$ and $\chi(X_2)$ are trivially obtained by summing the Euler characteristics of the corresponding vertices. \square

Example 3.9 *Consider the connectivity graph shown in Figure 1(a). Deleting the vertex associated with \mathcal{C}_1 and the two emanating edges shows that the inside of \mathcal{C}_1 is $\mathcal{I}(\mathcal{C}_1) = \mathcal{S}_1$ while the outside is $\mathcal{O}(\mathcal{C}_1) = \mathcal{S}_2 \cup \mathcal{C}_2 \cup \mathcal{S}_3$. Similarly, deleting the vertex associated with \mathcal{C}_2 and the two emanating edges shows that the inside of \mathcal{C}_2 is $\mathcal{I}(\mathcal{C}_2) = \mathcal{S}_1 \cup \mathcal{C}_1 \cup \mathcal{S}_2$ while the outside is $\mathcal{O}(\mathcal{C}_2) = \mathcal{S}_3$.*

Two ovals are said to be *nested* if their insides intersect. Moreover, an oval \mathcal{C} is *nested* in another oval \mathcal{C}' if $\mathcal{I}(\mathcal{C}) \subset \mathcal{I}(\mathcal{C}')$. The *topological type* of a curve corresponds with the number of ovals and their nesting structure, e.g., see [7], which can be determined directly from the output of Algorithm 3 in light of Theorem 3.8.

Example 3.10 From Example 3.9, since $\mathcal{I}(\mathcal{C}_1) \cap \mathcal{I}(\mathcal{C}_2) = \mathcal{S}_1 = \mathcal{I}(\mathcal{C}_1)$, this shows that \mathcal{C}_1 and \mathcal{C}_2 are nested. In fact, $\mathcal{I}(\mathcal{C}_1) \subset \mathcal{I}(\mathcal{C}_2)$ shows that \mathcal{C}_1 is nested in \mathcal{C}_2 .

Example 3.11 For the connectivity graph shown in Figure 1(b), $\mathcal{I}(\mathcal{C}_1) = \mathcal{S}_1$ and $\mathcal{I}(\mathcal{C}_2) = \mathcal{S}_3$ showing that \mathcal{C}_1 and \mathcal{C}_2 are not nested since $\mathcal{I}(\mathcal{C}_1) \cap \mathcal{I}(\mathcal{C}_2) = \emptyset$.

4 Dividing type for curves

For a homogeneous polynomial $f \in \mathbb{R}[x_0, x_1, x_2]$ such that $C(f)$ is smooth, the following determines the *dividing type* of f . In particular, f is *non-dividing* if $C(f) \setminus C_{\mathbb{R}}(f)$ is connected, and *dividing* otherwise. The key to the proposed computation, which addresses a problem stated in [7], is to represent the Riemann surface $C(f)$ as a surface in a real affine space where $C_{\mathbb{R}}(f)$ is a curve that lies on this surface so that Algorithm 1 can be used. The following describes using Whitney's embedding [13] of \mathbb{P}^2 into \mathbb{R}^7 to accomplish this.

Each point $(x_0, y_0, x_1, y_1, x_2, y_2) \in \mathbb{S}^5$ yields $[x_0 + iy_0, x_1 + iy_1, x_2 + iy_2] \in \mathbb{P}^2$ where $i = \sqrt{-1}$. Each fiber of this map from \mathbb{S}^5 to \mathbb{P}^2 corresponds with a circle. In particular, if $(x_0, y_1, x_1, y_1, x_2, y_2) \in \mathbb{S}^5$, for every $(\alpha, \beta) \in \mathbb{S}^1$, one has

$$\begin{aligned} [x_0 + iy_0, x_1 + iy_1, x_2 + iy_2] &= [(\alpha + i\beta)(x_0 + iy_0), (\alpha + i\beta)(x_1 + iy_1), (\alpha + i\beta)(x_2 + iy_2)] \\ &= [(\alpha x_0 - \beta y_0) + i(\beta x_0 + \alpha y_0), (\alpha x_1 - \beta y_1) + i(\beta x_1 + \alpha y_1), (\alpha x_2 - \beta y_2) + i(\beta x_2 + \alpha y_2)] \in \mathbb{P}^2 \end{aligned}$$

and

$$(\alpha x_0 - \beta y_0, \beta x_0 + \alpha y_0, \alpha x_1 - \beta y_1, \beta x_1 + \alpha y_1, \alpha x_2 - \beta y_2, \beta x_2 + \alpha y_2) \in \mathbb{S}^5.$$

One way to identify all such points is via Whitney's embedding [13] $W : \mathbb{S}^5 \mapsto \mathbb{R}^7$ defined by

$$W(x_0, y_0, x_1, y_1, x_2, y_2) = \begin{bmatrix} x_1 x_2 + y_1 y_2 \\ y_1 x_2 - x_1 y_2 \\ x_0 x_2 + y_0 y_2 \\ x_0 y_2 - y_0 x_2 \\ x_0 x_1 + y_0 y_1 \\ y_0 x_1 - x_0 y_1 \\ x_0^2 + y_0^2 - x_1^2 - y_1^2 \end{bmatrix}$$

since one can easily check that, for every $(\alpha, \beta) \in \mathbb{S}^1$,

$$W(x_0, y_0, x_1, y_1, x_2, y_2) = W(\alpha x_0 - \beta y_0, \beta x_0 + \alpha y_0, \alpha x_1 - \beta y_1, \beta x_1 + \alpha y_1, \alpha x_2 - \beta y_2, \beta x_2 + \alpha y_2).$$

For $U_{\mathbb{R}} = W(\mathbb{S}^5) \subset \mathbb{R}^7$, $U_{\mathbb{R}}$ is an embedding of \mathbb{P}^2 into \mathbb{R}^7 and defining equations for $U_{\mathbb{R}}$ can be obtained via elimination

$$\langle W(x_0, y_0, x_1, y_1, x_2, y_2) - u, x_0^2 + y_0^2 + x_1^2 + y_1^2 + x_2^2 + y_2^2 - 1 \rangle \cap \mathbb{R}[u] = \mathbb{R}[u_1, \dots, u_7] \quad (7)$$

yielding a defining set of 20 cubic polynomials in $\mathbb{R}[u]$. In particular, the vanishing of these 20 cubics yields an irreducible variety $U \subset \mathbb{C}^7$ of dimension 4 and degree 6 such that $U_{\mathbb{R}} = U \cap \mathbb{R}^7$. Moreover, $\mathbb{P}_{\mathbb{R}}^2$ corresponds with $y_0 = y_1 = y_2 = 0$ which, via the map W , embeds as the two-dimensional subset $U_{\mathbb{R}} \cap V_{\mathbb{R}}(u_2, u_4, u_6) = U_{\mathbb{R}} \cap V_{\mathbb{R}}(u_2^2 + u_4^2 + u_6^2) \subset \mathbb{R}^7$.

Now, to embed $C(f)$ into \mathbb{R}^7 , one simply determines polynomials $f_{\mathbb{R}}$ and $f_{\mathbb{I}}$ from f such that

$$f(x_0 + iy_0, x_1 + iy_1, x_2 + iy_2) = f_{\mathbb{R}}(x_0, y_0, x_1, y_1, x_2, y_2) + if_{\mathbb{I}}(x_0, y_0, x_1, y_1, x_2, y_2). \quad (8)$$

The vanishing of f on \mathbb{P}^2 corresponds with the vanishing of $f_{\mathbb{R}}$ and $f_{\mathbb{I}}$ on $(x_0, y_0, x_1, y_1, x_2, y_2) \in \mathbb{S}^5$ which W then embeds in \mathbb{R}^7 as a surface in $U_{\mathbb{R}}$. That is, defining equations for $C(f)$ embedded into \mathbb{R}^7 , which by abuse of notation will also be called $C(f)$, is obtained from (7) via

$$\left\langle \begin{array}{l} W(x_0, y_0, x_1, y_1, x_2, y_2) - u, x_0^2 + y_0^2 + x_1^2 + y_1^2 + x_2^2 + y_2^2 - 1, \\ f_{\mathbb{R}}(x_0, y_0, x_1, y_1, x_2, y_2), f_{\mathbb{I}}(x_0, y_0, x_1, y_1, x_2, y_2) \end{array} \right\rangle \cap \mathbb{R}[u] = \mathbb{R}[u_1, \dots, u_7]. \quad (9)$$

In particular, by assumption on f , $C(f) \subset \mathbb{R}^7$ is a smooth surface. The curve $C_{\mathbb{R}}(f)$, by abuse of notation, will be viewed as the curve embedded into \mathbb{R}^7 defined by $C(f) \cap V_{\mathbb{R}}(u_2, u_4, u_6) = C(f) \cap V_{\mathbb{R}}(u_2^2 + u_4^2 + u_6^2)$. This immediately yields an approach for computing the dividing type.

Theorem 4.1 *Suppose that $f \in \mathbb{R}[x_0, x_1, x_2]$ such that $C(f) \in \mathbb{P}^2$ is smooth. Let $f_{\mathbb{R}}$ and $f_{\mathbb{I}}$ be as in (8) and $f_1, \dots, f_\ell \in \mathbb{R}[u]$ be a generating set of polynomials obtained from (9). Thus, $F = \{f_1, \dots, f_\ell\}$ defines a surface $V_{\mathbb{C}}(F)$, where $V_{\mathbb{R}}(F)$, which corresponds with the embedding of $C(f)$ in \mathbb{R}^7 , is a smooth subset of $V_{\mathbb{C}}(F)$. Moreover, the dividing type of $C(f) \setminus C_{\mathbb{R}}(f)$ is equivalent to the dividing type of $V_{\mathbb{R}}(F) \setminus V_{\mathbb{R}}(F, u_2^2 + u_4^2 + u_6^2) \subset \mathbb{R}^7$. In particular, for random $c \in \mathbb{R}^7$ and*

$$r(u) = \frac{u_2^2 + u_4^2 + u_6^2}{(1 + (u_1 - c_1)^2 + \dots + (u_7 - c_7)^2)^2}, \quad (10)$$

Algorithm 1 using F and r correctly computes the number of connected components of $C(f) \setminus C_{\mathbb{R}}(f)$ with probability one, which is either 1 and f is non-dividing, or 2 and f is dividing.

Proof. Since $C(f) \subset \mathbb{P}^2$ is a Riemann surface, $V_{\mathbb{R}}(F) \subset \mathbb{R}^7$ is a smooth subset of $V_{\mathbb{C}}(F)$ since $V_{\mathbb{R}}(F)$ is the embedding of $C(f)$ into \mathbb{R}^7 . Moreover, in \mathbb{R}^7 , $\mathbb{P}_{\mathbb{R}}^2$ is obtained by the simultaneous vanishing of u_2 , u_4 , and u_6 so that $C_{\mathbb{R}}(f)$ in \mathbb{R}^7 corresponds with

$$V_{\mathbb{R}}(F) \cap V_{\mathbb{R}}(u_2, u_4, u_6) = V_{\mathbb{R}}(F, u_2^2 + u_4^2 + u_6^2).$$

Therefore, $C(f) \setminus C_{\mathbb{R}}(f)$ embeds into \mathbb{R}^7 as $V_{\mathbb{R}}(F) \setminus V_{\mathbb{R}}(F, u_2^2 + u_4^2 + u_6^2)$. The last statement using Algorithm 1 follows from [5, Thms. 3.4 & 4.4]. \square

Example 4.2 *As an illustration, consider $f(x_0, x_1, x_2) = x_0x_2 - x_1^2$. Since f has degree 2 and $C_{\mathbb{R}}(f)$ has the maximum number of connected components, namely $1 + \binom{2-1}{2} = 1$, f is known to be dividing [8]. The following verifies this using Theorem 4.1. From f , one computes*

$$f_{\mathbb{R}}(x_0, y_0, x_1, y_1, x_2, y_2) = x_0x_2 - x_1^2 - y_0y_2 + y_1^2 \quad \text{and} \quad f_{\mathbb{I}}(x_0, y_0, x_1, y_1, x_2, y_2) = x_0y_2 + x_2y_0 - 2x_1y_1.$$

Using (9), one obtains that $C(f) \subset \mathbb{R}^7$ is a surface of degree 8 defined by the following 11 quadratics:

$$\begin{array}{ll} f_1 = 2u_1u_6 - 2u_5u_6 - u_4u_7, & f_2 = 3u_4u_5 + 3u_3u_6 + u_2u_7 - u_6u_7 + u_6, \\ f_3 = 3u_3u_5 - 3u_4u_6 - u_1u_7 + u_5u_7 - u_5, & f_4 = 2u_2u_5 - 2u_5u_6 - u_4u_7, \\ f_5 = u_1u_5 - u_5^2 - u_2u_6 + u_6^2 + u_3u_7, & f_6 = u_3^2 + u_4^2 - u_5^2 - 2u_2u_6 + u_6^2 + u_3u_7, \\ f_7 = 3u_2u_3 + 3u_1u_4 - 2u_2u_7 - u_6u_7 + u_6, & f_8 = 3u_1u_3 - 3u_2u_4 + 2u_1u_7 + u_5u_7 - u_5, \\ f_9 = 2u_2^2 - 3u_5^2 + 2u_2u_6 - u_6^2 - u_7^2 + u_3 + u_7, & f_{10} = 2u_1u_2 + 4u_5u_6 + u_4u_7 + u_4, \\ & f_{11} = 2u_1^2 + u_5^2 + 2u_2u_6 - 5u_6^2 - 2u_3u_7 - u_7^2 - u_3 + u_7. \end{array}$$

For simplicity of presentation, we took $c = (-1, 1/5, -3/4, 1/3, 2/3, -3/2, -4/3)$ and applied Algorithm 1 to $F = \{f_1, \dots, f_{11}\}$ and r as in (10). This produced 4 routing points, three of index 0 and

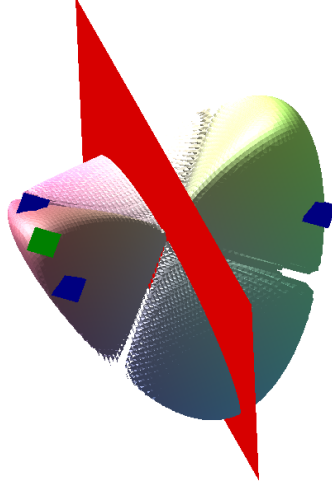


Figure 7: Visualization of $C(f)$ in Example 4.2 projected onto $(u_1, u_2, u_3) \in \mathbb{R}^3$ with the plane corresponding to $u_2 = 0$ dividing the surface into two connected components. The 3 routing points of index 0 are blue while the routing point of index 1 is green.

one of index 1, which decomposes into two connected components with each having Euler characteristic 1. In fact, one connected component corresponds with a single routing point of index 0 while the other corresponds to the remaining routing points: two of index 0 and one of index 1. Figure 7 illustrates the projection of $C(f)$ onto $(u_1, u_2, u_3) \in \mathbb{R}^3$ where the plane corresponding to $u_2 = 0$ cuts the surface into two connected components where the index 0 routing points are shown in blue and the index 1 is in green. In particular, this shows that $C(f) \setminus C_{\mathbb{R}}(f)$ consists of two connected components verifying that f is dividing.

Two challenges with using Theorem 4.1 are computing the generating set for the elimination ideal in (9) and then computing routing points for this typically overdetermined system. Another approach is use the original system with one modification as follows. Upon fixing the routing function r as in (10), there are finitely-many routing points that we need to compute. As mentioned above, the fibers of W are circles. Hence, for a general linear form $L(x_0, y_0, x_1, y_1, x_2, y_2)$, i.e., a homogeneous linear polynomial, L vanishes at exactly two points in each fiber over the finitely-many routing points. Letting

$$r_n(u) = u_2^2 + u_4^2 + u_6^2 \quad \text{and} \quad r_d(u) = 1 + (u_1 - c_1)^2 + \cdots + (u_7 - c_7)^2,$$

we have $r(u) = r_n(u)/r_d(u)^2$. For simplicity of presentation, let $x = (x_0, y_0, x_1, y_1, x_2, y_2)$ and

$$G(u, x) = \begin{bmatrix} W(x) - u \\ S(x) \\ f_{\mathbb{R}}(x) \\ f_{\mathbb{I}}(x) \\ L(x) \end{bmatrix}. \quad (11)$$

Then, the corresponding critical point system associated with $r(u)$ on $G(u, x) = 0$ is the following

system on $(u, x, \alpha, \lambda) \in \mathbb{C}^7 \times \mathbb{C}^6 \times \mathbb{C}^2 \times \mathbb{P}^{11}$ constructed using (homogenized) Lagrange multipliers:

$$\mathcal{G}(u, x, \alpha, \lambda) = \begin{bmatrix} G(u, x) \\ 1 - \alpha_1 r_n(u) \\ 1 - \alpha_2 r_d(u) \\ \lambda \begin{bmatrix} \nabla(r_n)\alpha_1 - 2\nabla(r_d)\alpha_2 \\ JG(u, x) \end{bmatrix} \end{bmatrix} \quad (12)$$

where the gradient vector and Jacobian matrix are taken with respect to (u, x) . In particular, \mathcal{G} is a well-constrained system with $26 = 7 + 6 + 2 + 11$ polynomials.

Corollary 4.3 *With the setup from Theorem 4.1 and randomly selected linear form L , for every routing point $u^* \in \mathbb{R}^7$, there exists $(x^*, \alpha^*, \lambda_+^*, \lambda_-^*) \in \mathbb{C}^6 \times \mathbb{C}^2 \times \mathbb{P}^{11} \times \mathbb{P}^{11}$ such that $(u^*, \pm x^*, \alpha^*, \lambda_\pm^*)$ are two distinct nonsingular solutions of $\mathcal{G} = 0$ as in (12) with probability one.*

Proof. With probability one, L transversely intersects the fibers of the finitely-many routing points in two distinct points. These points are nonzero since $S(x) = 0$ implies $x \neq 0$. Moreover, from (11), $G(u, x) = 0$ if and only if $G(u, -x) = 0$. For each routing point $u^* \in \mathbb{R}^7$, there must exist $x^* \in \mathbb{C}^6 \setminus \{0\}$ such that x^* and $-x^*$ are the two distinct solutions of $G(u^*, x) = 0$. Since $u^* \in \mathbb{R}^7$, $r_d(u^*) \neq 0$ with $\alpha_2^* = r_d(u^*)^{-1}$. Similarly, since u^* is a routing point, $r(u^*) \neq 0$ yielding $r_n(u^*) \neq 0$ with $\alpha_1^* = r_n(u^*)^{-1}$. Hence, $\alpha^* = (\alpha_1^*, \alpha_2^*) = (r_n(u^*)^{-1}, r_d(u^*)^{-1})$. Finally, since the system \mathcal{G} is constructed to compute the critical points of $r(u)$ on $G(u, x) = 0$, there exists Lagrange multipliers $\lambda_+^* \in \mathbb{P}^{11}$ and $\lambda_-^* \in \mathbb{P}^{11}$ associated with (u^*, x^*, α^*) and $(u^*, -x^*, \alpha^*)$, respectively. Finally, transversality of L and nondegeneracy of routing points ensures that each $(u^*, \pm x^*, \alpha^*, \lambda_\pm^*)$ is a nonsingular solution of $\mathcal{G} = 0$. \square

From $W(x) - u$, one can trivially eliminate u and $(\lambda_1, \dots, \lambda_7)$ to reduce to a well-constrained system with $26 - 14 = 12$ polynomials on $\mathbb{C}^6 \times \mathbb{C}^2 \times \mathbb{P}^4$. Additionally, one could intrinsically solve on $L(x) = 0$ to remove another equation and variable, and also dehomogenize λ via $\lambda_0 = 1$ due to the smoothness assumption.

Remark 4.4 *Satisfying $\mathcal{G} = 0$ is a necessary condition for critical points of r on $C(f)$. However, there can be additional solutions which are not critical points. The number of such additional solutions is independent of the generic choice of L , but the actual solutions themselves are dependent on L . Such additional solutions can be easily discarded since the last coordinate of the corresponding Lagrange multipliers will be nonzero. Of course, one way to avoid these additional solutions would be to add the condition $\lambda_{11} = 0$ into \mathcal{G} , but this would yield an overdetermined system while \mathcal{G} is already well-constrained and routing points already correspond with nonsingular isolated solutions.*

Example 4.5 *For a general homogeneous polynomial f of degree d , Table 1 considers solving $\mathcal{G} = 0$ for $1 \leq d \leq 6$ using Bertini [2]. In particular, for $1 \leq d \leq 6$, the number of extraneous solution pairs as in Remark 4.4 is d^2 while the number of critical points is much larger. Hence, if one solves $\mathcal{G} = 0$ directly, this data suggests that the amount of extra computation associated with the extraneous solutions is small compared with the computation associated with the critical points. Moreover, one can compute the critical points associated with a given polynomial of degree d using a parameter homotopy [10] that deforms from a general f to the given polynomial. With such a parameter homotopy, one does not need to consider the extraneous solutions and only needs to track one path associated with each critical pair.*

d	$\#V_{\mathbb{C}}(\mathcal{G})$	$\#$ critical pairs	$\#$ extraneous pairs
1	22	10	1
2	152	72	4
3	522	252	9
4	1288	628	16
5	2670	1310	25
6	4932	2430	36

Table 1: Summary of solutions of $\mathcal{G} = 0$ for a general polynomial f of degree d

To illustrate, consider the setup from Example 4.2. From Table 1, one needs to track 72 paths using a parameter homotopy and then sort through the set of endpoints to determine the routing points. In particular, for these 72 paths, 50 converged with four corresponding to routing points. Of course, these are the same four routing points obtained in Example 4.2 and illustrated in Figure 7.

After computing the routing points using \mathcal{G} as in (12), one can also determine the connected components as in Algorithm 1 as follows. Although the choice of linear form L in G in (11) was chosen randomly in Corollary 4.3 to ensure transversality associated with every routing point simultaneously, one can perform the gradient ascent (since r in (10) is always positive) using a localized version of L that is updated along the trajectory, i.e., L can be chosen to be real and transverse on a local part of the trajectory. For example, a linear form L that will work locally near x^* is $L(x) = v^* \cdot x$ where v^* is a unit vector perpendicular to x^* . In order to determine the correct number of components, one simply considers only the coordinates u , i.e., identifies $(u^*, x^*, \alpha^*, \lambda_+^*)$ and $(u^*, -x^*, \alpha^*, \lambda_-^*)$.

5 Examples

The following considers some additional examples to demonstrate the new methods. All computations of routing points were performed using Bertini [2] and trajectories computed using Matlab.

5.1 Two tori in space

As highlighted in Remark 3.7, connectivity graphs can be computed for hypersurfaces in higher dimensions with the following considering two surfaces in $\mathbb{P}_{\mathbb{R}}^3$ which are both homeomorphic to the torus as described in [11, § 4.1]. In particular, consider

$$\begin{aligned} f_1(x) &= (x_1^2 + x_2^2 + x_3^2 + 3x_0^2)^2 - 16x_0^2(x_1^2 + x_2^2), \\ f_2(x) &= 10(x_1^2 + x_2^2 - x_3^2 - 1)(x_1^2 + x_2^2 + x_3^2 + 1) + x_3^4. \end{aligned}$$

The first is directly from [11, § 4.1] while the second is constructed as described in [11, § 4.1] as a perturbation of the union of a one-sheeted hyperboloid and an imaginary quadric.

For illustration purposes, with $c = (1/2, -1/3, -1/5, 1/7)$, $V_{\mathbb{R}}(f_1, S)$ has 8 routing points with two connected components that are identified under the antipodal action each with 4 routing points: one of index 0, two of index 1, and one of index 2. Thus, each connected component of $V_{\mathbb{R}}(f_1, S)$ has Euler characteristic 0 and the same holds for the corresponding component in \mathbb{P}^3 .

Using the same c , $V_{\mathbb{R}}(S) \setminus V_{\mathbb{R}}(f_1, S)$ yields 12 routing points and three connected components, two of which are identified under the antipodal action and the other is invariant. All have Euler

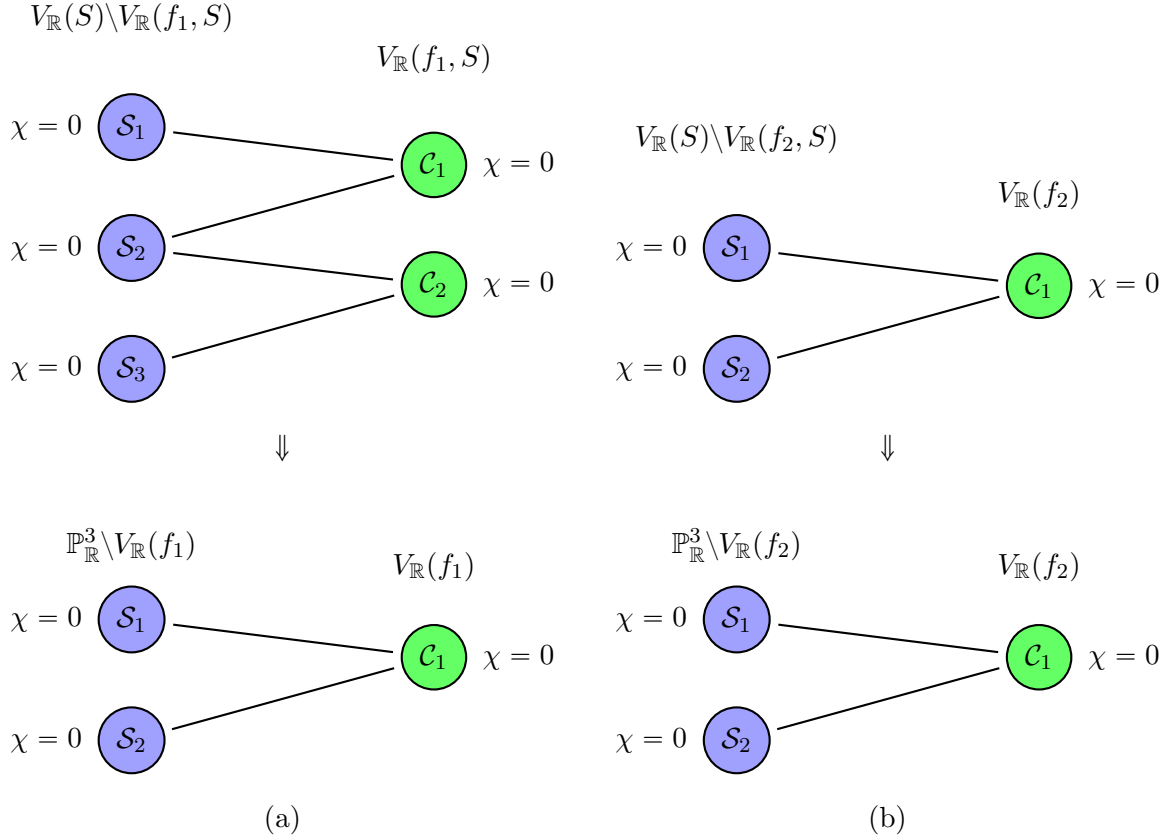


Figure 8: Connectivity graph for two tori in $\mathbb{P}_{\mathbb{R}}^3$.

characteristic 0. In fact, the invariant one corresponds with a set of 8 routing points: three of index 0, four of index 1, and one of index 2. Each of the other two connected components in \mathbb{S}^3 correspond with a set of 2 routing points having index 0 and index 1. Figure 8(a) shows the corresponding connectivity graphs in \mathbb{S}^3 and $\mathbb{P}_{\mathbb{R}}^3$. As expected, this verifies that the Euler characteristic of both \mathbb{S}^3 and $\mathbb{P}_{\mathbb{R}}^3$ are 0.

Similarly, for $V_{\mathbb{R}}(f_2, S)$, there are 4 routing points with a single connected component that is invariant under the antipodal action. The indices of the routing points are as follows: one of index 0, two of index 1, and one of index 2. For $V_{\mathbb{R}}(S) \setminus V_{\mathbb{R}}(f_2, S)$, there are also 4 routing points and two connected components that are invariant under the antipodal action. Each connected component has two routing points having index 0 and index 1. As above, each connected component has Euler characteristic 0. Figure 8(b) shows the corresponding connectivity graphs in \mathbb{S}^3 and $\mathbb{P}_{\mathbb{R}}^3$.

5.2 Hyperbolic sextic

Consider the hyperbolic sextic

$$f(x) = 6(x_1^2 + x_2^2 - x_0^2)(x_1^2 + x_2^2 - 2x_0^2)(x_1^2 + x_2^2 - 3x_0^2) + x_1^3 x_2^3$$

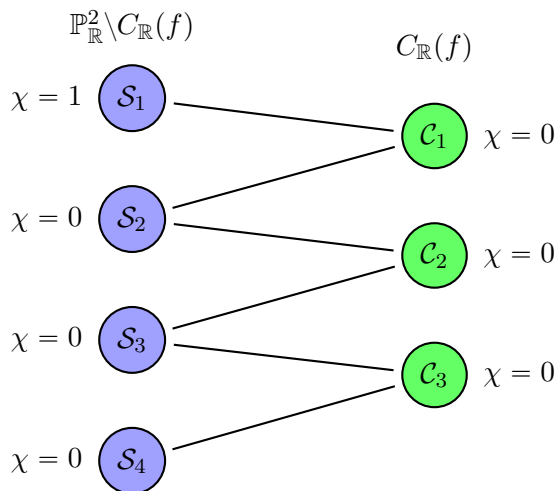


Figure 9: Bipartite connectivity graph arising in $\mathbb{P}_{\mathbb{R}}^2$ for hyperbolic sextic.

from [7] which is dividing with three nested ovals. As observed in [7, Fig. 1], this is the maximal nesting for sextics. The following verifies the nesting structure and dividing type.

Using Algorithm 3, the connectivity graph is shown in Figure 9. In particular, $C_{\mathbb{R}}(f)$ has three ovals \mathcal{C}_1 , \mathcal{C}_2 , and \mathcal{C}_3 with

$$\mathcal{I}(\mathcal{C}_1) = \mathcal{S}_1 \subset \mathcal{I}(\mathcal{C}_2) = \mathcal{I}(\mathcal{C}_1) \cup \mathcal{C}_1 \cup \mathcal{S}_2 \subset \mathcal{I}(\mathcal{C}_3) = \mathcal{I}(\mathcal{C}_2) \cup \mathcal{C}_2 \cup \mathcal{S}_3.$$

Hence, \mathcal{C}_1 is nested in \mathcal{C}_2 which is nested in \mathcal{C}_3 .

From Theorem 4.1 and Corollary 4.3, for a fixed but randomly selected $c \in \mathbb{R}^7$, there were 36 routing points on $C(f) \setminus C_{\mathbb{R}}(f)$: 9 with index 0 and 27 with index 1. A visualization from applying Algorithm 1 to determine the connected components is provided in Figure 10. In particular, there are two connected components: one corresponds with 5 routing points of index 0 and 14 routing points of index 1, while the other corresponds with 4 routing points of index 0 and 13 routing points of index 1. Hence, both connected components in \mathbb{R}^7 have Euler characteristic -9 . Since $C(f) \setminus C_{\mathbb{R}}(f)$ has two connected components, f is dividing.

6 Conclusion

By using routing functions on real algebraic varieties in real affine space following [5], several algorithms were proposed for performing computations on real projective hypersurfaces. For hypersurfaces in $\mathbb{P}_{\mathbb{R}}^n$, an algorithm was described for computing the connectivity graph, which is a bipartite graph that describes the relationship between connected components of the hypersurface and connected components of its complement. Such a graph naturally determines the one-sided and two-sided components of the hypersurface. Moreover, for the curve case, this graph completely describes the nesting structure of the two-sided components, called ovals, and thus the topological type of the curve. These computations were performed via the double cover provided by \mathbb{S}^n in which one needs to identify antipodal points. Routing functions naturally provide a membership test which is used to determine which components in \mathbb{S}^n are identified under the antipodal map.

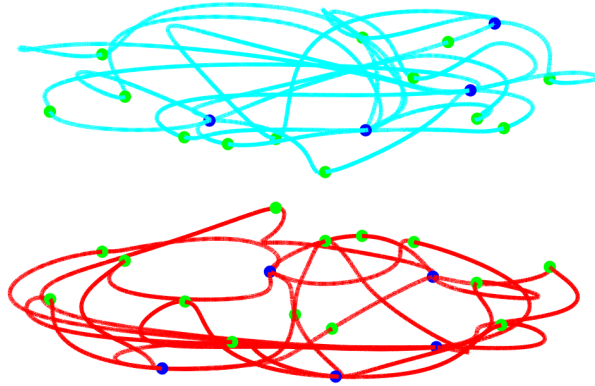


Figure 10: Visualization of the 36 routing points and gradient ascent paths on $C(f) \setminus C_{\mathbb{R}}(f)$ in terms of the (u_2, u_4, u_6) coordinates. The 9 routing points of index 0 are blue while the 27 routing points of index 1 are green. The gradient ascent paths are colored red and cyan to distinguish between the two connected components of $C(f) \setminus C_{\mathbb{R}}(f)$.

A problem stated in [7] is to develop a computational approach for determining the dividing type of a smooth curve C in \mathbb{P}^2 . The approach presented in Theorem 4.1 and Corollary 4.3 uses Whitney's embedding [13] of \mathbb{P}^2 into \mathbb{R}^7 and then a routing function [5] to determine the dividing type.

Several examples were used to demonstrate the numerical approaches for performing these aforementioned computations associated with real projective hypersurfaces.

Acknowledgments

The authors thank Thomas Brazelton, Joseph Cummings, and Raluca Vlad for discussions surrounding real connected components. Both authors were supported in part by National Science Foundation grants CCF 2331400. The first author was supported in part by the Robert and Sara Lumkins Collegiate Professorship and Simons Foundation SFM-00005696. The second author was supported in part by the Arthur J. Schmitt Presidential Leadership Fellowship.

References

- [1] S. Basu, R. Pollack, and M.-F. Roy. *Algorithms in Real Algebraic Geometry*, volume 10 of *Algorithms and Computation in Mathematics*. Springer-Verlag, Berlin, second edition, 2006.
- [2] D. J. Bates, J. D. Hauenstein, A. J. Sommese, and C. W. Wampler. Bertini: Software for numerical algebraic geometry. Available at bertini.nd.edu.
- [3] J. Bochnak, M. Coste, and M.-F. Roy. *Real Algebraic Geometry*, volume 36 of *Ergebnisse der Mathematik und ihrer Grenzgebiete (3)*. Springer-Verlag, Berlin, 1998.
- [4] C. Brown. Constructing cylindrical algebraic decomposition of the plane quickly. Available at <https://www.usna.edu/Users/cs/wcbrown/research/MOTS2002.1.pdf>, 2002.

- [5] J. Cummings, J. D. Hauenstein, H. Hong, and C. D. Smyth. Smooth connectivity in real algebraic varieties. *Numerical Algorithms*, to appear.
- [6] A. Harnack. Ueber die Vieltheiligkeit der ebenen algebraischen Curven. *Math. Ann.*, 10(2):189–198, 1876.
- [7] N. Kaihnsa, M. Kummer, D. Plaumann, M. Sayyary Namin, and B. Sturmfels. Sixty-four curves of degree six. *Exp. Math.*, 28(2):132–150, 2019.
- [8] C. Kalla and C. Klein. Computation of the topological type of a real Riemann surface. *Math. Comp.*, 83(288):1823–1846, 2014.
- [9] A. Lerario and E. Lundberg. Statistics on Hilbert’s 16th problem. *Int. Math. Res. Not. IMRN*, 2015(12):4293–4321, 2015.
- [10] A. P. Morgan and A. J. Sommese. Coefficient-parameter polynomial continuation. *Appl. Math. Comput.*, 29(2):123–160, 1989.
- [11] O. Viro. Mutual position of hypersurfaces in projective space. In *Geometry of differential equations*, volume 186 of *Amer. Math. Soc. Transl. Ser. 2*, pages 161–176. Amer. Math. Soc., Providence, RI, 1998.
- [12] O. Viro. From the sixteenth Hilbert problem to tropical geometry. *Jpn. J. Math.*, 3(2):185–214, 2008.
- [13] H. Whitney. The self-intersections of a smooth n -manifold in $2n$ -space. *Ann. of Math. (2)*, 45:220–246, 1944.
- [14] G. Wilson. Hilbert’s sixteenth problem. *Topology*, 17(1):53–73, 1978.